Numerical Study of the Noise Generation by a Rifle Shooting with Suppressor

Lo, Shi-Wei[1], Tai, Chang-Hsien[1], Teng, Jyh-Tong[2], and Lin, Yong-Jhou[1]

[1] Department of Vehicle Engineering, National Pingtung University of Science and Technology, Pingtung, 91201 Taiwan, R.O.C.
[2] Department of Mechanical Engineering, Chung Yuan Christian University, Chung-Li, 32023, Taiwan, R.O.C.

1 Abstract

The moving bullet out of a rifle barrel is propelled by a fired explosive charge. A disturbed muzzle blast wave is initiated which lasts several milliseconds. The supersonic bullet causes an acoustic shock wave that propagates away from the bullet's moving path. Besides, the muzzle blast is a main acoustic source to far field receivers. The noise generated by blast waves was investigated in this paper. Axial symmetry, unsteady, Large Eddy Simulation (LES), and Ffowcs-Williams and Hawkins (FW-H) equations were solved by the implicit-time formulation. For the spatial discretization, second order upwind scheme was employed. In addition, dynamic mesh model was used to where the ballistic domain changed with time due to the motion of bullet. Results obtained for muzzle flow field and for noise recorded were compared with those obtained from experimental data; these two batches of results were in agreement. In this study, three cases of gunshot including an unsuppressed rifle and two models of suppressors were simulated. Besides, serial images of species distributions and velocity vectors-pressure contours in suppressors and near muzzle field were displayed. The sound pressure levels (dB) in far field that were post-processed by the fast Fourier transform (FFT) were compared. The proposed physical model and the numerical simulations used in the present work are expected to be extended to solve other shooting weapon problems with three-dimensional and complex geometries.

2 Introduction

To a rifle in battle field, especially to a sniper, acoustic attenuation in shooting is very important. In a rifle shooting, muzzle blast wave caused by the discharged gas is a main acoustic source for analysis to far field receivers. The sudden discharge is generally fuel-rich and mixes with air turbulently entrained from the surroundings [1]. While a bullet is passing through the muzzle, a main shock wave attached on the bullet is generated during its flight at supersonic velocity. The discharged propellant gas generates a normal wave and an oblique shock wave. The main shock and air disturbance in both regions are the acoustic sources which cause the receivers to hear about the noises [2]. In order to trap the expanding gases that create the loud supersonic crack of a fired bullet, a sound suppressor is

Correspondence to: swlo@mail.npust.edu.tw

attached to the muzzle of a firearm. The installations of muzzle blast suppressors are to minimize the sound emanating from a rifle upon discharge, in order to avoid shooter's detection by enemy forces [3]. In past decades, a great deal of efforts had been devoted to understanding the mechanism of muzzle flow fields [4]. As a practical rule, the impulse noise of small calibre weapons is concentrated in the frequency range of 500-1000 Hz while the ones of large calibre weapons and explosions are in the low-frequency range of less than 200 Hz [5]. Many researches dedicated to study the design of suppressors to attenuate noise by changing the frequency of gunshot noise [6]. In fact, sounds have much lower energy than fluid flows. It is a great challenge to predict each flow phenomenon and to simulate sound waves numerically. The purpose of this study was to optimize the design of noise attenuation. Axial symmetry, unsteady, LES and FW-H equations were solved by the implicit-time formulation. For the spatial discretization, two-order upwind scheme was employed. Dynamic mesh model also was applied to the ballistic domain which shifted with time. Results obtained for the muzzle flow field and for the far field noise were compared with those obtained from experimental shadow photographs and measurements; these two batches of results were in agreement. Furthermore, the present computational predictions revealed clearly the detailed shock waves propagations/interactions inside the suppressor models and around the muzzle region. These results were detailed by the pressure time histories at recorded locations in each suppressor model as well as pressure contours and velocity vectors in the suppressor. It is noted that muzzle flows with species concentrations were also analyzed. The far field noises, described by sound pressure levels (dB) and frequencies (Hz), generated by gunshots were also compared.

3 Mathematical Formulation

A gunshot generates complex physical phenomena, which involves chemical reactions induced by the discharged gases. This transient flow and acoustic are characterized by shock propagation, interaction, reflection, and disturbance around the muzzle and are affected by the species of propellant and structure of suppressors. Although the time duration of the present problem is very short, to calculate the noise generated by the pressure disturbance, the viscous effects are considered. The axial, viscid flow is described in its conservation form by the Navier–Stokes equations.

3.1 Numerical Method

The present numerical code utilizes the cell-averaged finite volume method. Considering the viscous effects, the Large Eddy Simulation (LES) turbulence model is used to resolve the large vortex structures in this study. In spatial discretization, the heat flux term is calculated by method of central differences. The upwind scheme with the flux of a cell's interface is presented as:

$$\varphi^i = \frac{1}{2}\left(\varphi^i(U_L)+\varphi^i(U_R)\right)-\frac{1}{2}\left|\hat{\varphi}\right|\left(U_R-U_L\right) = \frac{1}{2}\left(\varphi^i(U_L)+\varphi^i(U_R)\right)-\frac{1}{2}\hat{R}\left(\hat{U}\right)\left|\hat{\Lambda}\right|\hat{R}^{-1}\left(\hat{U}\right)\left(U_R-U_L\right) \qquad (1)$$

where U_L and U_R are the conservative variables at left and right sides of the cell interface, respectively. $\phi^i(U_L)$ and $\phi^i(U_R)$ are for calculating the flux between two sides of cell interface. $\left|\hat{\phi}\right|$ is a Jacobian matrix of $\phi(U)$, and $\hat{R}\left(\hat{U}\right)$ is the right characteristic matrix of $\left|\hat{\phi}\right|$. $\left|\hat{\Lambda}\right|$ is a diagonal matrix that consists of characteristic lines. The characteristic velocities are $\hat{u}_q - \hat{c}$, $\hat{u}_q$, and $\hat{u}_q + \hat{c}$, where "^" means the value calculated by Roe's average formula. Cell interface value is obtained by using second-order accuracy of the extrapolation method. The cell interface value is determined from the extrapolation method using a second-order weighted approximation.

For transient simulations, temporal discretization involved the integration of every term in the differential equations over a time step. Considering the unconditionally stable with respect to time step size, the fully implicit scheme was used in this study. The implicit time integration of the transient terms was used and the first-order backward differences accurate temporal discretization is given as:

$$\frac{\phi^{n+1}-\phi^{n}}{\Delta t}=F(\phi^{n+1}) \quad (2)$$

where ϕ is scalar quantity, n and n+1 are values at the current and next time levels, t and t+Δt, respectively.

3.2Moving mesh conservation equations

In this study, the moving mesh model was employed in the movement of bullet during gunshot simulations. Upon release, the bullet moves as a result of the pressure differential; the six degree of freedom was used to compute this coupled motion, and the layering scheme from the dynamic mesh model was utilized. The integral form of the conservation equation for a general scalar, ϕ, on an arbitrary control volume, V , whose boundary was moving, can be written as:

$$\frac{d}{dt}\int_V \rho\phi dV+\int_{\partial V}\rho\phi(\vec{u}-\vec{u}_g)\cdot d\vec{A}=\int_{\partial V}\Gamma\nabla\phi\cdot d\vec{A}+\int_V S_\phi dV \quad (3)$$

where ρ is the fluid density, $\vec{u}$ is the flow velocity vector, $\vec{u}_g$ is the grid velocity of the moving mesh, Γ is the diffusion coefficient, and S_ϕ is the source term of ϕ.

To preserve the flow precision around the bullet, the fitted meshes were used around the bullet. And the other ones along trajectory (interface region) construed with uniform structure meshes. By using moving mesh model, the boundary conditions on both ends of chamber and trajectory were assumed unmovable. Additionally, mesh sizes on both ends could be adjusted with the interface region moving. On the left side, the meshes enlarged until reaching the limited size which is one and half times larger than the original size. Otherwise, the meshes would be compressed until the size is less than half of the original size. Multi-block, conformal, unstructured meshes (adjoined to the projectile and in suppressor) and uniform meshes along the moving trace were adopted.

3.3 Acoustic analogy model

In this study, an attempt was made to predict both the flow field and emitted sound of gunshot in far field. Owing to the supersonic flow field, the equations were solved on the basis of compressibility. The present simulation attempted to capture this flow field by LES turbulence model with moving mesh system. The sound propagation was calculated also by the Ffowkes-Williams and Hawkings analogy [7]. Although expending more computing source, LES turbulence model was applied in the prediction of the pressure fluctuations. The mechanism of the aerodynamic noise radiation is revealed. The noise is mainly radiated from the muzzle and bullet, generating strong vortices and shock.
The Ffowcs Williams and Hawkings (FW-H) equation adopted Lighthill's acoustic analogy to predict the sound generated by the acoustic sources from muzzle blast.

$$\frac{1}{a_0{}^2}\frac{\partial^2 p'}{\partial t^2}-\nabla^2 p'=\frac{\partial^2}{\partial x_i\,\partial x_j}\{T_{ij}H(f)\}-\frac{\partial}{\partial x_i}\{[P_{ij}n_j+\rho u_i(u_n-v_n)]\delta(f)\}+\frac{\partial}{\partial t}\{[\rho_0 v_n+\rho(u_n-v_n)]\delta(f)\} \quad (4)$$

where u_i and v_i are fluid velocity components in the x_i direction. u_n and v_n are normal to the surface f = 0. $\delta(f)$ is Dirac delta function and H(f) is Heaviside function. p' is sound pressure at the far field and is presented as: $p' = p-p_0$.

4 Proof of numerical algorithms

To compare the muzzle flow structures, numerical simulation was completed by the experimental shadowgraph [8]. The schematic flow evolutions outside the barrel were calculated over a 1.5 ms time interval, as shown in Fig. 1. The barrel shock was modeled, but with a slightly different shape than that of the experimental data. The barrel shock and free-shear layer, vortex structure, the slipstream were modeled with this CFD simulation.

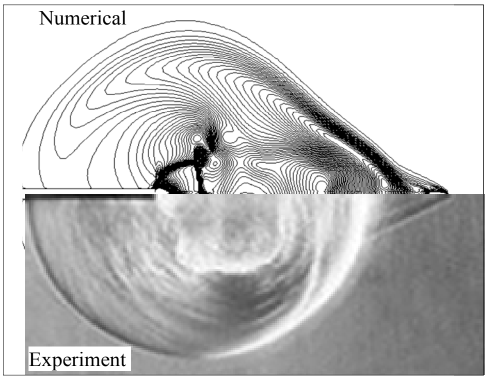

Figure 1 Comparison of muzzle flow structures between numerical simulation- isopycnics and experimental results [8]

5 Results and Discussions

In this study, a bullet was initially resting adjacent to the chamber where the pressure and temperature were patched up to 200 atm and 1500 K, while the ambient air pressure and temperature was 1 atm and 300 K, respectively. Three cases were simulated by solving the finite volume method for axial-symmetric, compressible, unsteady, viscous flow.

5.1 Illustration of geometry

A schematic illustration of different suppressors and boundary conditions is displayed in Fig. 2. The chamber, bullet, barrel, and suppressor were assumed to be non-slip and isotherm rigid surfaces. The inner diameter of the tubular sleeves is 4 cm, total length of tubular body is 15 cm, and the length of barrel is 50 cm. The domain of calculation is 4-m × 0.5-m (length × height).

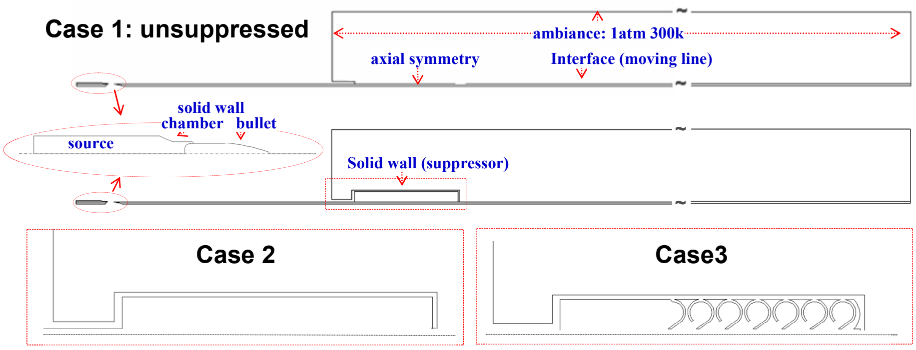

Figure 2 Schematic diagrams of different suppressors and boundary conditions

5.2 Shock wave structures of muzzle flow field by species distribution

Series images of species distributions of muzzle flow field in Case 1 with gunshot of unsuppressed rifle are displayed in Fig. 3. The development of flow structure includes jet flow, propagations, interactions, collisions, dissipation, and vortex, displayed at 0.82, 1.0, 1.5, 2.0 2.5 and 3.0 ms. The high pressure and temperature gas ejected from the barrel, expanded radially and formed a typical jet flow structure, as shown in Fig. 3(a). However, the obstruction by the axially moving bullet caused the ejecting angle to be larger than typical muzzle jet flow at muzzle region. Besides, the strong discharged gas interacted with the ambient air and generated disturbance and vortex which caused the noise, as shown in Figs. 3(b) ~ 3(f). Subsequently, the bullet moved away from muzzle; the jet flow still injected and interacted with surround air until its strength scattered.

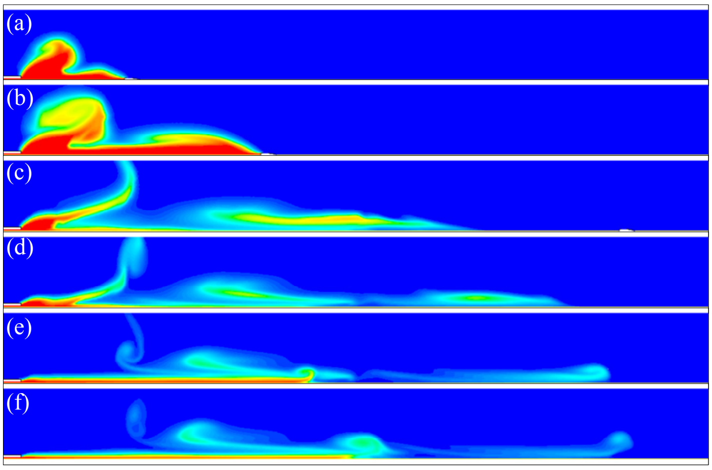

Figure 3 Series numerical images of species distributions near muzzle region by the gunshot of unsuppressed rifle in Case 1: (a) 0.82 ms (b) 1.00 ms (c) 2.00 ms (d) 3.00 ms.

5.3 Shock wave structures in suppressors and muzzle flow field

While the bullet was passing through muzzle and entering the suppressor, the precursor still moved in front of the bullet head and the discharged gas was ejected into the suppressor radically, forming a shock wave, as shown in Fig. 4(a) and 4(b). Furthermore, the air close to the muzzle of suppressor was pushed outward and a vortex was formed around its surface and the incident gas in suppressor still interacted with reverse flow and delayed the exit flow of suppressor, as shown in Fig. 4(c) and 4(d).

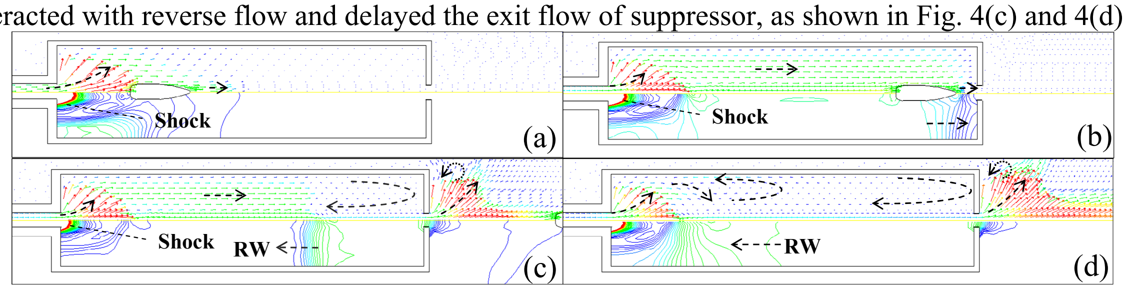

Figure 4 Distributions of pressure and velocity vectors in Case2
(a) 0.72 ms (b) 0.80 ms (c) 0.86 ms (d) 0.90 ms

In Case 3, the design of the front space was to mitigate the impact of discharged gas and to shift the noise frequency. In Fig. 5 (a) and 5(b), the air was pushed by the high pressure discharged gas and was flowing backwards. In Figs. 5(c) and 5(d), the jet flow interacted with the air and generated a vortex near the suppressor.

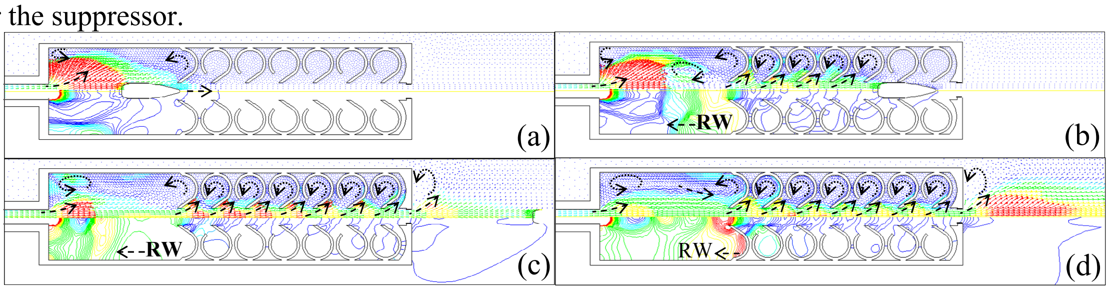

Figure 5 Distributions of pressure and velocity vectors in Case 3
(a) 0.72 ms (b) 0.80 ms (c) 0.86 ms (d) 0.90 ms

5.4 Comparison of noise with different suppressor

The noise in Case2 was lowest (16 dB at 4 m and 20 dB at 128 m) than those in Case 1, as shown in Fig. 6(a). The sound pressure levels were different for various assigned receivers at logistic lengths from 4 m to 128 m. The sound pressure level (dB) in Case 1 showed higher peaks and were centralized in 400~2000 Hz, as shown in Fig. 6(b). While an expansion chamber was attached on the rifle in Case 2, the sound pressure levels were reduced, as shown in Fig. 6(c). In Case 3, arrangements in the chambers were responsible for causing the shock waves to cancel each other, resulting in a reduction in noise. Besides, the sensitive region (which is around 1,000~3,000 Hz) of noise frequencies is avoided by these designs, as shown in Figs. 6(d).

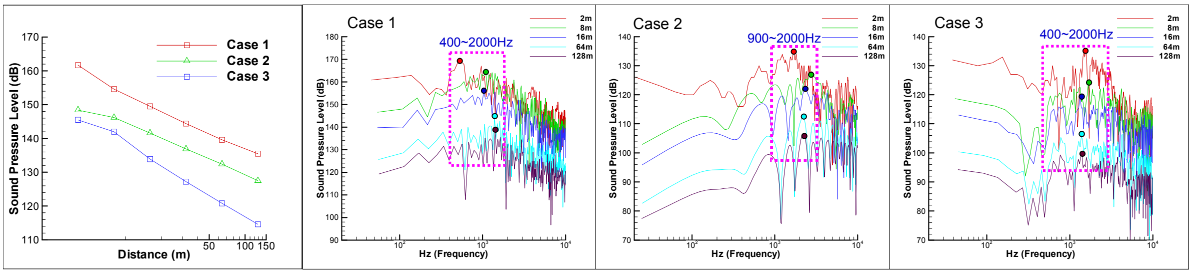

(a) (b) (c) (d)

Figure 6 Comparison of sound pressure level (a) and (b)~(d)spectral analysis of pressure signals

6 Conclusions

The impulse noise methodology was employed to analyze and compare the noise attenuation properties of suppressors. The muzzle flow field of rifle shooting was validated with experimental results. The LES and species transport models were useful to provide the acoustic source. The F-W H model was also useful to calculate SPL in far field. Changing the suppressor could shift the frequency and decrease the noise in gunshot. It is difficult to obtain absolute SPL predictions in 2D or axial domain due to the need to estimate the correlation length of turbulent flow structures in the spanwise direction. The proposed physical model and the numerical simulations used in the present work can be extended to solve other shooting weapon problems with three-dimensional and complex geometries.

References

[1] Klingenberg, G., "Gun Muzzle Blast and Flash," Propellants, Explosives, Pyrotechnics, Vol. 14, Issue 2, 1989, pp. 57–68.

[2] Wang, J. C. T. and Widhopf, G.. F. "Numerical Simulation of Blast Flowfields Using A High Resolutin TVD Finite Volume Scheme," Computers & Fluids Vol. 18. No. 1, 1990, pp.103-137.

[3] Koenig, B.E., Hoffman, S.M., Nakasone, H., and Beck, S.D. "Signal Convolution of Recorded Free-field Gunshot Sounds," Journal of Audio Engineering Society., vol. 46(7/8), pp. 634-653, July/Aug 1998.

[4] Cler, D. L., Chevaugeon, N., Shephard, M. S., Flaherty, J. E. and Remacle, J. F. "Computational Fluid Dynamics Application to Gun Muzzle Blast- A Validation Case Study," Technical Report ARCCB-TR-03011, 2003.

[5] Pääkkönen, R." Noise Attenuation of Structures Against Impulses from Large Calibre Weapons or Explosions," Applied Acoustics 45 (1995), pp. 263-218.

[6] Pääkkönen, R., " Environmental noise reduction means of weapons," Acoustic 08 Pairs, 2008, pp. 5811-5814.

[7] Ffowcs-Williams, J. E. and Hawkings, D. L., " Sound Generation by Turbulence and Surfaces in Arbitrary Motion," Proc. Roy. Soc. London, A264, pp.321-342, 1969.

[8] Settles, G., "High-speed Imaging of Shock Waves, Explosions and Gunshots," American Scientist, Volume 94, Number 1, 2006, pp.22-31.